Eur Biophys J (2002) 31: 378–382
DOI 10.1007/s00249-002-0228-0

ARTICLE

Bradley C. Steel · Marcela M. Bilek
David R. McKenzie · Cristobal G. dos Remedios

A technique for microsecond heating and cooling of a thin (submicron) biological sample

Received: 17 January 2002 / Revised: 14 March 2002 / Accepted: 14 March 2002 / Published online: 13 June 2002

Abstract Temperature excursions of short duration are useful in exploring the effects of stress on biological systems. Stress will affect the conformation of biological molecules such as proteins, which will lead to an effect on their function. The feasibility of generating such temperature excursions is demonstrated by solving the heat diffusion equation for an aqueous layer on a silicon wafer. The silicon is rapidly heated by a laser pulse and also acts as a heat sink to quench the temperature rise. An oxide layer was used to limit the maximum temperature attained by the sample. We show that exposures above a 50 °C benchmark can be confined to times less than 5 μs.

Keywords Laser temperature jump · Heat diffusion equation · Microwave radiation · Temperature pulse

Introduction

The proliferation of non-ionizing radiation sources, particularly microwave sources, in the telecommunications industry has led to an increased interest in the biological effects of microwave radiation. It is well known that such radiation causes temperature rises that have adverse effects on the functions of macromolecules like proteins (Durney 1985; Reilly 1998; Repacholi and Cardis 1997). A number of researchers have reported biological effects in the absence of a *measurable* temperature rise (Belyaev et al. 2000; Cao et al. 1995; Donellan et al. 1997; Harvey and French 1999; Repacholi et al. 1997). Experiments using both continuous (CW) (Daniells et al. 1998) and pulsed (J.A. Laurence, personal communication) microwave sources have demonstrated that athermal microwave exposure activates the heat shock response. This is defined as the way the cell responds at the molecular level to external stressors, such as toxins or extreme temperatures. Activation of the heat shock response is a strong indicator that microwave sources cause partial unfolding of proteins within cells. There remains a need for further research into the biological effects of microwave radiation in the absence of a measurable temperature rise.

Calculations by Laurence et al. (2000) showed that a protein molecule is in thermal equilibrium with its surroundings on the time scales required for unfolding, since the energy of vibrational modes dissipates rapidly. Because of this, it was suggested that protein unfolding is induced by transient heating of the molecule and its local environment. Microwaves are likely to cause "hotspots" in particular parts of a cell, such as the membrane (Liu and Cleary 1995). Such localized absorption could result in transient temperature rises which would not be *measurable*, but would be sufficient to induce protein unfolding (Laurence et al. 2000).

Analysis of this hypothesis requires knowledge of the duration of a temperature rise required to cause a conformational change in a protein. Experimental work using laser temperature-jumps (T-jumps) and fluorescence or Raman monitoring has set a timescale for the unfolding of the protein backbone in the sub-microsecond range (Lednev et al. 1999; Thompson et al. 1997).

A determination of the length of time required for a transient temperature excursion to permanently affect protein structure requires an experimental arrangement capable of both heating and cooling on a nano/micro timescale.

Presented at the Australian Biophysical Society Meeting, 2001

B.C. Steel (✉) · M.M. Bilek · D.R. McKenzie
School of Physics, University of Sydney,
Sydney 2006, Australia
E-mail: bsteel@physics.usyd.edu.au
Tel.: +61-2-93515980
Fax: +61-2-93517725

C.G. dos Remedios
Institute for Biomedical Research,
Muscle Research Unit, University of Sydney,
Sydney 2006, Australia

Materials and methods

Exposure system

A number of conditions were identified as necessary to facilitate rapid cooling. These were:

1. Heating of a small volume.
2. Proximity to a relatively large heat sink.
3. Good thermal conduction.
4. Large temperature jumps.

It is difficult to accurately measure in situ temperature in small volumes over short timescales. Accordingly, the temperature excursions were determined using a computer simulation.

A design that satisfies the above requirements is presented in Fig. 1. The system is illuminated using a frequency-doubled Nd-YaG laser, with a 5 ns pulse length. The laser pulse passes through the coverslip and "aqueous solution", and is absorbed by the silicon layer. A coating, such as silicon dioxide, can be deposited between the silicon surface and the aqueous solution. Since the volume heated is more than 100 times as wide as it is thick, modelling this system involves a one-dimensional solution to the heat diffusion equation. This allows the simulation to be reasonably quick and accurate.

Modelling of temperature

A finite-element analysis technique was used to model the temperature distribution. The system was broken into thin slabs, each with a characteristic thickness and composition. Each slab was assumed to be composed of either silicon, water, or glass, and to have a particular temperature representing the centre of the slab. Thermal conductivities and heat capacities were calculated at this temperature using a linear interpolation between published values. To reduce calculation time, after modelling the first microsecond of thermal conduction, the values of the heat capacity and thermal conductivity were not calculated for each iteration. To preserve accuracy, they were recalculated before the associated error reached 0.1% for any slab. This was small compared to uncertainties in the published parameters.

Heat conduction between identical slabs, of thickness l, can be calculated using the following formula:

$$Q/A = k\Delta T\Delta t/l, \quad \Delta t \text{ small} \tag{1}$$

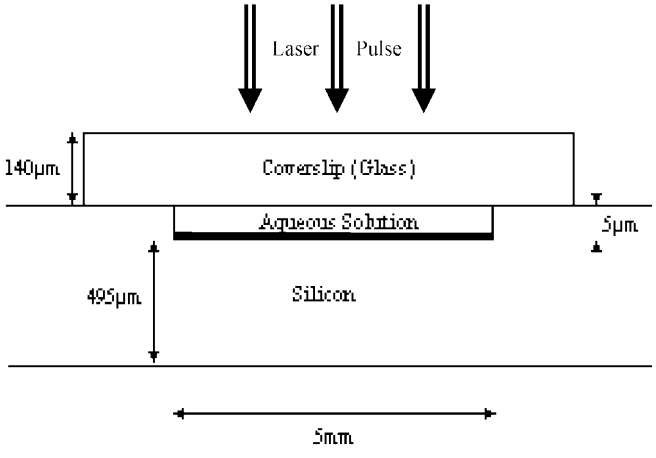

Fig. 1. Diagram (not to scale) of the experimental apparatus used for the laser pulse experiments. A 1 μm silicon oxide layer (indicated by the *heavy line*) was deposited on the top of a recess in the silicon in contact with an aqueous solution

where Q is the heat conducted, A is the contact area, k is the thermal conductivity, ΔT is the temperature difference between the slabs and Δt is the time during which heat is conducted.

In general, for slabs with different thermal conductivities and thicknesses, this is modified to:

$$Q_{ij}/A = 2k_ik_j\Delta T\Delta t/\left(k_il_j + k_jl_i\right) \tag{2}$$

where subscripts i and j denote the i-th and (neighbouring) j-th slabs.

The temperature rise of a slab is then determined using:

$$T_i(t+\Delta t) - T_i(t) = \sum_{j=i\pm1} Q_{ij}/Al_ic\rho \tag{3}$$

where the summation is performed using both neighbouring slabs, c is the heat capacity per unit mass, and ρ is the density.

We assumed an adiabatic boundary on the top glass surface, and a 20 °C heat reservoir at the lower silicon surface. These conditions had minimal effect on the modelling results, since the heat did not diffuse significantly to the boundaries during the time period for which modelling was performed.

The initial conditions placed the system at room temperature (20 °C), and assumed room temperature absorption of 532 nm light in silicon. For water and glass, absorption at this wavelength is small enough that no significant temperature rise occurs (< 1 mK). Heat absorption was assumed to occur uniformly over a 5 ns period. Losses due to reflection at each interface were included by reducing the absorbed energy accordingly.

The calculations were performed in MATLAB, which uses matrix methods to improve calculation efficiency. Convergence of the finite element analysis method was checked by doubling the number of slabs (from 300 to 600) and shortening the time steps from 25 ps to 2.5 ps. This produced a temperature distribution identical to within 1% of the temperature change, throughout 70 μs of simulation.

Evaluation of thermal conductivity and heat capacity

Thermal conductivities and heat capacities for the materials used are known up to their melting points. Simple modelling demonstrated that both the silicon and water layers reached temperatures exceeding their melting points. However, experiments with pulse energies up to 10^4 J m^{-2} showed no evidence of water evaporation, while multiple exposures at this energy resulted in fracturing of the coverslip, indicating bulk evaporation. This suggests that superheating of the water occurred for energies less than 10^4 J m^{-2}. Similar observations were made for silicon, with surface melting observed under SEM for energies well above 10^4 J m^{-2}, and slight surface modification at energies near this value (see Fig. 2). This represents the upper energy limit for accurate modelling.

Thermal conductivities and heat capacities are known for superheated water. Values up to 370 °C were obtained from Vargaftik et al. (1996). Since continuation of the trend in these data results in unphysical conditions (such as negative conductivity, or unrealistically high heat capacity), thermal properties above 370 °C were set equal to those at 370 °C. Similarly, properties were held constant for the other materials at temperatures above that for which thermal properties are available. These are presented in Fig. 3.

Pressure differences should equalize on a nanosecond timescale. Given that features observed in modelling are on a microsecond timescale, thermal properties used assume constant atmospheric pressure.

Results

Figure 4 presents the temperature distributions in the water layer at 0.5, 1, 2, 5 and 10 μs after a 2×10^3 J m^{-2} laser pulse. The successive curves show the water-silicon

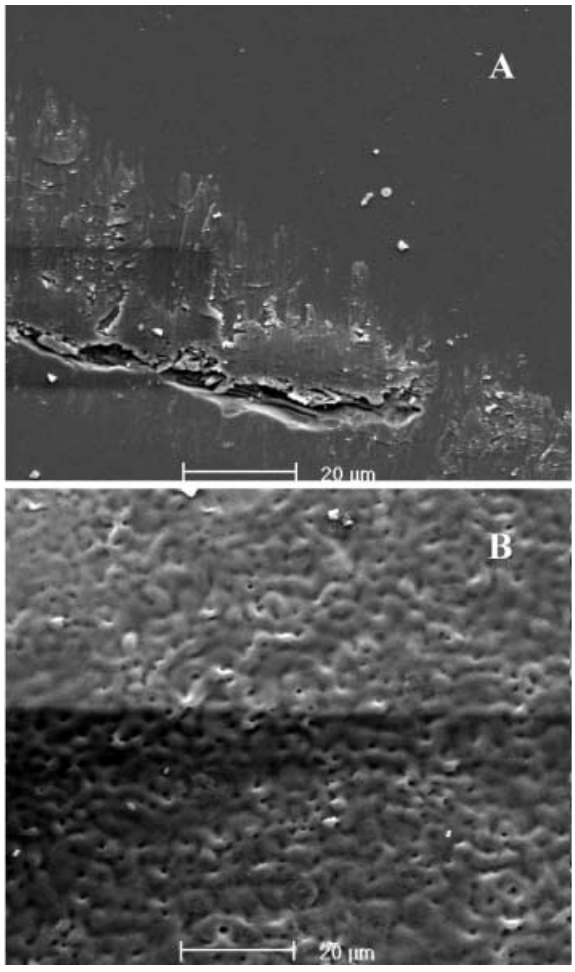

Fig. 2A, B. SEM images of the surface of a silicon wafer, following laser exposure in the setup described in Fig. 1. **A** follows a single 10^4 J m^{-2} laser pulse (crystallographic orientation 110). This displays a fractured region of the wafer (note there is no surface modification of areas distant from the fracture). No evidence of melting was present. **B** follows 20 pulses at a 10 Hz repetition rate (crystallographic orientation 100). Repeated pulsing was used to simulate the effects of greater temperature excursions (and thus higher pulse powers), each pulse heating the entire region by 6 °C per pulse. Under these conditions the water layer partially evaporated after 3–6 pulses, and the surface shows evidence of melting. Fractures similar to those illustrated in **A** were also observed (not shown)

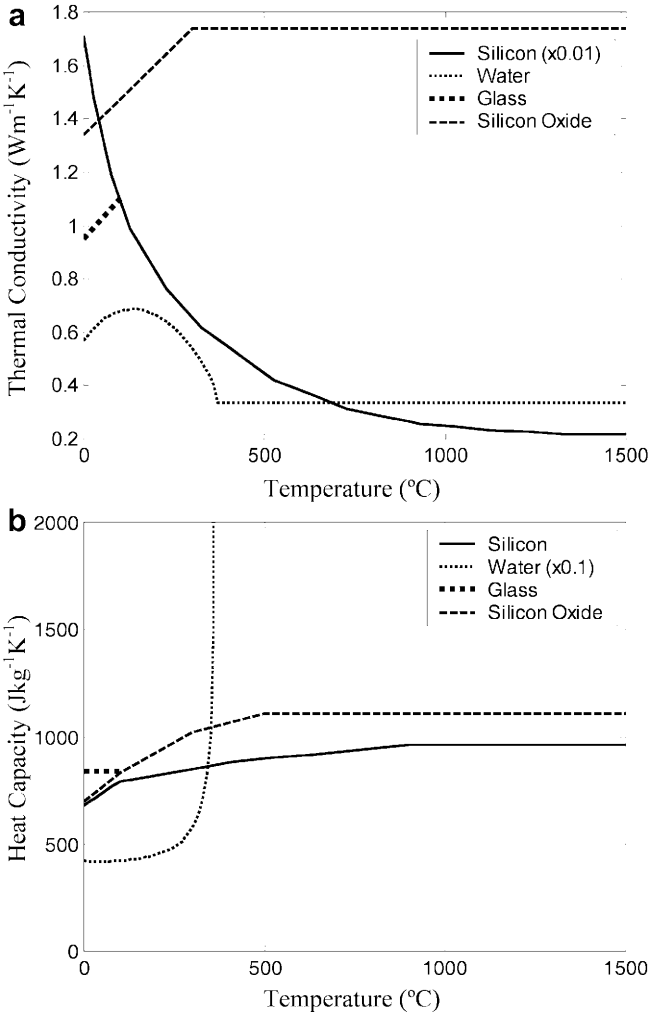

Fig. 3. **a** Thermal conductivities and **b** heat capacities of materials used in the simulation. At temperatures above which published values are available, the last published value was used. Values for glass are plotted only in the 0–100 °C range, since glass did not exceed this temperature during modelling. The thermal conductivity of silicon is 100 times the values plotted in **a**, and the heat capacity of water is 10 times the values plotted in **b** (Kaye and Laby 1995; Lide 1999; Raznjevic 1976; Vargaftik et al. 1996)

interface cooling, and some of the heat diffusing from the heated silicon into the water layer. Clearly, the temperature profile of the water layer is highly non-uniform. However, the region near the surface demonstrates rapid cooling, dropping below 100 °C in 0.4 μs, and below 60 °C within 2 μs. At this pulse energy, the maximum surface temperature reached in the silicon is approximately 600 °C.

Clearly, higher pulse energies produce a greater temperature increase, and vice versa. However, the temperature profiles are very similar regardless of pulse energy, although their magnitudes are different. This is true up to pulse energies around 5×10^3 to 10×10^3 J m^{-2}, where deviations become noticeable. Notably, approximately equal volumes of water are heated in all cases. Figure 5 plots the temperature profile of the slab of water in contact with the silicon as a function of time. This approximates the average temperature through a 50 nm slab centred 25 nm above the silicon surface.

The uneven temperature profile throughout the water layer suggests that this technique would be useful in circumstances either where an assay was available to measure effects on only a small fraction of the exposed macromolecules (those which happen to be in the heated region), or where the macromolecules were fixed at a precise distance from the silicon surface.

Figure 6A presents the temperature profile over time 0.5 μm from the silicon surface for pulse energies of 2, 2.5 and 3×10^3 J m^{-2}. At this distance, there is no large initial temperature spike. If a layer of macromolecules

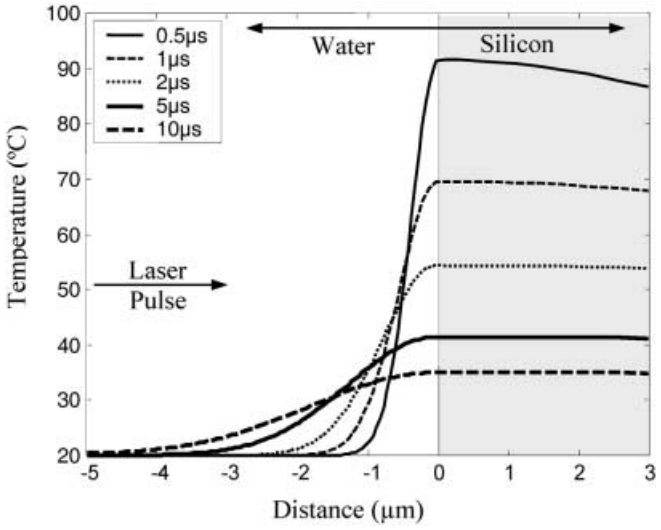

Fig. 4. Modelled temperature distributions in a water layer and the top 3 μm of the silicon surface, at 0.5, 1, 2, 5 and 10 μs after a 2000 J m^{-2} laser pulse

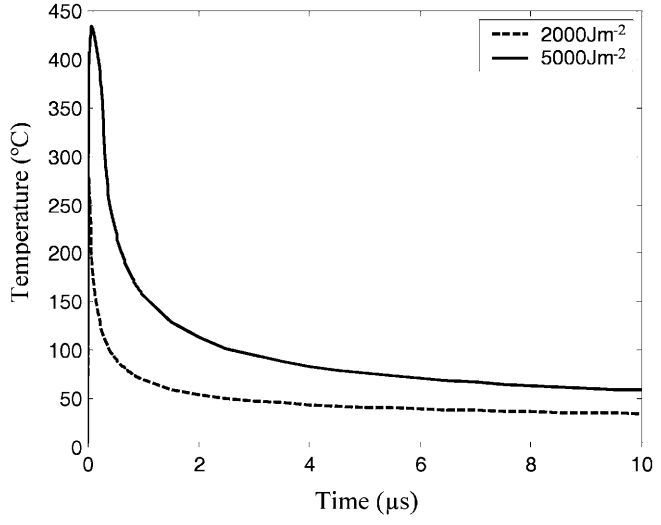

Fig. 5. Modelled temperature distributions in the water in contact with silicon over a time of 10 μs. In modelling, each slab of water, at the centre of which temperature is calculated, is 50 nm thick. This plot shows the average temperature through the 50 nm slab closest to the silicon surface. The two cases plotted are for heating pulses of 2000 J m^{-2} (*lower curve*) and 5000 J m^{-2} (*upper curve*). The relatively large time taken for the latter case to cool below 300 °C is a result of the high values of heat capacity of water above 370 °C

(such as a protein) could be fixed at this distance from the silicon surface, then by varying the input power, the time for which the protein is heated above a reference temperature can be varied. This presents a unique means of varying the timescale over which a protein is heated above a reference temperature. Note that the maximum temperature and the duration of the exposure are both linked to the pulse power.

In general, fixing a layer of macromolecules a known distance from the silicon surface will require a new layer

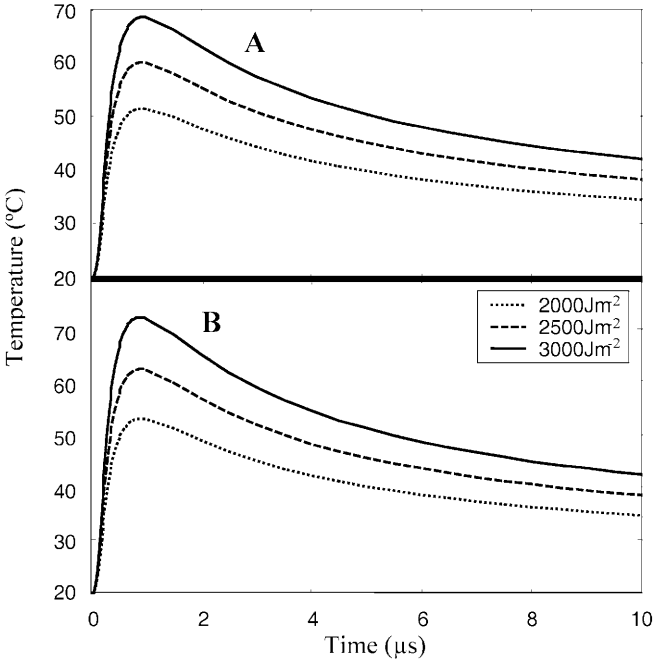

Fig. 6. Modelled temperature distributions over time in water **A** 0.5 μm from the silicon surface with no oxide layer present and **B** at the water interface of a 1 μm silicon oxide layer placed on the silicon surface. In both **A** and **B**, three cases are plotted over 10 μs for heating pulses of 2000 J m^{-2}, 2500 J m^{-2} and 3000 J m^{-2}. The *reference line* at 50 °C is an arbitrary temperature at which a protein may change conformation

to be placed between those macromolecules and the surface. This layer may be either an aqueous solution or a thin solid layer with properties different to those of water. Silicon dioxide layers are commonly used in the semiconductor industry as a highly adherent, electrically insulating layer. A thin layer of silicon dioxide can be grown on the silicon and macromolecules can be bound to this surface. Such a layer could be created with any desired thickness up to approximately 5 μm by growth under wet conditions (Meindl et al. 1977), and should remain adherent following thermal shock.

Figures 6B and 7 demonstrate the temperature profiles with the presence of an oxidized layer one micron thick. As in Figs. 4 and 6A, the temperature profile at the oxide surface has a cooling time of ~5 μs, and the time taken to drop below a reference temperature can be varied by changing the laser power. For a protein that unfolds at a critical temperature of 50 °C, Fig. 6 shows that using a maximum temperature between 53 °C and 72 °C, any exposure time in the range 1–5 μs can be obtained. This timescale remains significantly slower than current estimates of protein unfolding rates (Lednev et al. 1999; Williams et al. 1996). However, these estimates are based on simple proteins, while proteins with intermediate structures will unfold more slowly. Note that the cooling rates are faster than obtained previously. Variations in oxide thickness will also have an effect on cooling rates, while reducing the initial temperature will decrease cooling times; that is, if

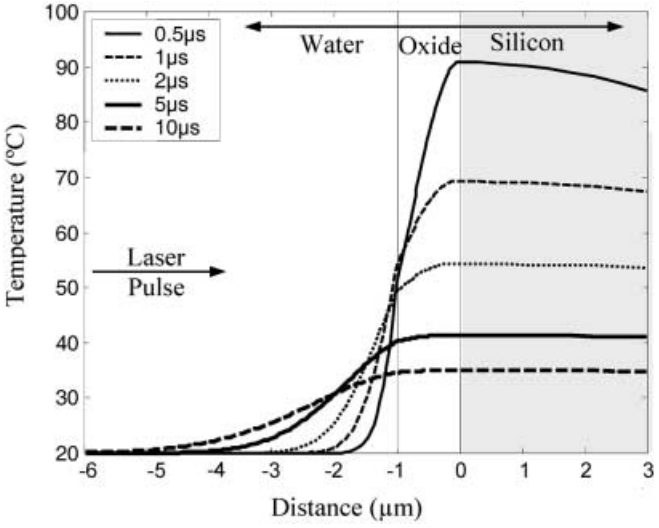

Fig. 7. Modelled temperature distributions in a water layer, a 1 μm silicon oxide layer, and the top 3 μm of the silicon surface. *Lines* represent the temperature at 0.5, 1, 2, 5 and 10 μs following a laser pulse of 2000 J m^{-2}

the system begins at 0 °C, then a temperature excursion to 53 °C would exceed 50 °C for only 0.6 μs.

Conclusions

The heating profile of a macromolecule on a silicon oxide surface can be controlled with maximum temperatures between 4 and 20 °C above a reference temperature, for periods of 1–5 μs. The magnitude and duration of the temperature excursion in an aqueous layer can be controlled by varying the laser power, surface oxide thickness, and initial temperature. Effects of temperature excursions on proteins could be analysed with techniques such as single molecule fluorescence resonance energy transfer (reviewed in dos Remedios and Moens, 1999) or motility assays (reviewed in Sellers 1999). Variations to the experiment described may allow cooling times in the sub-microsecond regime.

Such temperature excursions may be used to study protein kinetics, and to assess the validity of the ''hot-spot'' hypothesis for microwave radiation. Other possible applications for this technique would be to study the effects of controlled temperature shocks on protein functionality or macromolecular interactions.

References

Belyaev IY, Shcheglov VS, Alipov ED, Ushakov ED (2000) Nonthermal effects of extremely high-frequency microwaves on chromatin conformation in cells in vitro – dependence on physical, physiological, and genetic factors. IEEE Trans Microwave Theor 48:2172–2179

Cao GH, Liu LM, Cleary SF (1995) Cell cycle alterations induced by isothermal 27 MHz radio-frequency radiation exposure. Bioelectrochem Bioenerget 37:131–140

Daniells C, Duce I, Thomas D, Sewell P, Tattersall J, de Pomerai D (1998) Transgenic nematodes as biomonitors of microwave-induced stress. Mutat Res Fund Mol Mech Mutat 399:55–64

Donellan M, McKenzie DR, French PW (1997) Effects of exposure to electro-magnetic radiation at 835 MHz on growth, morphology and secretory characteristics of a mast cell analog, RBL-2H3. Cell Biol Int 21:427–439

dos Remedios CG, Moens PDJ (1999) Resonance energy transfer in proteins. In: Andrews DL, Demidov AA (eds) Resonance energy transfer. Wiley, Chichester, UK, pp 1–64

Durney CH (1985) The physical interactions of radiofrequency radiation fields and biological systems. In: The impact of proposed radio frequency radiation standards on military operations. (AGARD lecture series no. 138) NATO Advisory Group for Aerospace Research and Development (AGARD), Paris

Harvey C, French PW (1999) Effects on protein kinase C and gene expression in a human mast cell line, HMC-1, following microwave exposure. Cell Biol Int 23:739–748

Kaye GWC, Laby TH (1995) Tables of physical and chemical constants, 16th edn. Longman, Harlow, UK

Laurence JA, French PW, Lindner RA, McKenzie DR (2000) Biological effects of electromagnetic fields – mechanisms for the effects of pulsed microwave radiation on protein conformation. J Theor Biol 206:291–298

Lednev IK, Karnoup AS, Sparrow MC, Asher SA (1999) Alpha-helix peptide folding and unfolding activation barriers: a nanosecond UV resonance Raman study. J Am Chem Soc 121:8074–8086

Lide RD (ed) (1999) CRC handbook of chemistry and physics: a ready-reference book of chemical and physical data, 79th edn. CRC Press, Boca Raton, USA

Liu L, Cleary SF (1995) Absorbed energy distribution from radiofrequency electromagnetic radiation in a mammalian cell model – effect of membrane-bound water. Bioelectromagnetics 16:160–171

Meindl JD, Dutton RW, Saraswat KC, Plummer JD, Kamins TI, Deal BE (1977) Silicon epitaxy and oxidation. In: Van de Wiele F, Engl WL, Jespers PO (eds) Process and device modelling for integrated circuit design. Noorhoff, Leyden, Netherlands

Raznjevic K (1976) Handbook of thermodynamic tables and charts. McGraw-Hill, Washington

Reilly JP (1998) Guidelines for limiting exposure to time-varying electric, magnetic, and electromagnetic fields. Health Phys 74:494–522

Repacholi MH, Cardis E (1997) Criteria for EMF health risk assessment. Radiat Prot Dosim 72:305–312

Repacholi MH, Basten A, Gebski V, Noonan D, Finnie J, Harris AW (1997) Lymphomas in Eμ-Pim1 transgenic mice exposed to pulsed 900 MHz electromagnetic fields. Radiat Res 147:631–640

Sellers JR (1999) Myosins, 2nd edn. Oxford University Press, Oxford

Thompson PA, Eaton WA, Hofrichter J (1997) Laser temperature jump study of the helix↔coil kinetics of an alanine peptide interpreted with a ''kinetic zipper'' model. Biochemistry 36:9200–9210

Vargaftik NB, Vinogradov YK, Yargan VS (1996) Handbook of physical properties of liquids and gases. Begell House, New York

Williams S, Causgrove TP, Gilmanshin R, Fang KS, Callender RH, Woodruff WH, Dyer RB (1996) Fast events in protein folding: helix melting and formation in a small peptide. Biochemistry 35:691–697